

# Towards agricultural soil carbon monitoring, reporting and verification through Field Observatory Network (FiON)

Olli Nevalainen<sup>1</sup>, Olli Niemitalo<sup>2</sup>, Istem Fer<sup>1</sup>, Antti Juntunen<sup>2</sup>, Tuomas Mattila<sup>3</sup>, Olli Koskela<sup>2</sup>, Joni Kukkamäki<sup>2</sup>, Layla Höckerstedt<sup>1</sup>, Laura Mäkelä<sup>4</sup>, Pieta Jarva<sup>4</sup>, Laura Heimsch<sup>1</sup>, Henriikka Vekuri<sup>1</sup>, Liisa Kulmala<sup>1,5</sup>, Åsa Stam<sup>1</sup>, Otto Kuusela<sup>1,6,7</sup>, Stephanie Gerin<sup>1</sup>, Toni Viskari<sup>1</sup>, Julius Vira<sup>1</sup>, Jari Hyväluoma<sup>2</sup>, Juha-Pekka Tuovinen<sup>1</sup>, Annalea Lohila<sup>1,6</sup>, Tuomas Laurila<sup>1</sup>, Jussi Heinonsalo<sup>5</sup>, Tuula Aalto<sup>1</sup>, Iivari Kunttu<sup>2</sup>, Jari Liski<sup>1</sup>

<sup>1</sup> Finnish Meteorological Institute, FMI, Helsinki, Finland

<sup>2</sup> Häme University of Applied Sciences, HAMK, Hämeenlinna, Finland

<sup>3</sup> Finnish Environment Institute, SYKE, Helsinki, Finland

<sup>4</sup> Baltic Sea Action Group, BSAG, Espoo, Finland

<sup>5</sup> University of Helsinki, Institute for atmospheric and Earth system research (INAR), forest sciences, Helsinki, Finland

<sup>6</sup> University of Helsinki, Institute for atmospheric and Earth system research (INAR), physics, Helsinki, Finland

<sup>7</sup> University of Amsterdam, Computational Science, Amsterdam, Netherlands

*Correspondence to:* (olli.nevalainen@fmi.fi)

**Abstract.** Better monitoring, reporting and verification (MRV) of the amount, additionality and persistence of the sequestered soil carbon is needed to understand the best carbon farming practices for different soils and climate conditions, as well as their actual climate benefits or cost-efficiency in mitigating greenhouse gas emissions. This paper presents our Field Observatory Network (FiON) of researchers, farmers, companies and other stakeholders developing carbon farming practices. FiON has established a unified methodology towards monitoring and forecasting agricultural carbon sequestration by combining offline and near real-time field measurements, weather data, satellite imagery, modeling and computing networks. FiON's first phase consists of two intensive research sites and 20 voluntary pilot farms testing carbon farming practices in Finland. To disseminate the data, FiON built a web-based dashboard called Field Observatory (v1.0, fieldobservatory.org). Field Observatory is designed as an online service for near real-time model-data synthesis, forecasting and decision support for the farmers who are able to monitor the effects of carbon farming practices. The most advanced features of the Field Observatory are visible on the Qvidja site which acts as a prototype for the most recent implementations. Overall, FiON aims to create new knowledge on agricultural soil carbon sequestration and effects of carbon farming practices, and provide an MRV tool for decision-support.

## 31 **1 Introduction**

32 Farmers are managing one of the largest carbon stocks on the planet where even relatively small additions are important for  
33 climate change mitigation. Accordingly, the international “soil carbon 4 per mille” initiative aims at raising the soil organic  
34 carbon content by 0.4 % per year by adopting carbon farming practices (Minasny et al. 2017). Carbon farming practices include  
35 methods, such as ~~reduced soil disturbance (reduced or zero tillage)~~, increasing carbon inputs (soil amendments, cover crops,  
36 residue management) and crop rotations. Such practices do not only have the potential to partially refill the global soil carbon  
37 stock that has lost 116 Pg carbon due to land cultivation (Sanderman et al., 2017), but they could also improve soil structure  
38 and health, and increase crop yields (Merante et al. 2017; Oldfield et al. 2018). Annual carbon sequestration rates for different  
39 management practices vary from 100 to 1000 kg C ha<sup>-1</sup> (Merante et al., 2017; Minasny et al., 2017). Detecting sequestration  
40 rates in this range is difficult with traditional empirical soil sampling designs due to large spatial variability of soil carbon  
41 content and small relative changes in the soil carbon stock due to individual management actions (VandenBygaart and Angers  
42 2006; Heikkinen et al. 2021). This calls for better monitoring, reporting and verification (MRV) of the amount, additionality  
43 and persistence of the sequestered soil carbon due to carbon farming practices.

44  
45 Towards this goal, we established the Field Observatory Network (FiON), a network of researchers, farmers, companies and  
46 other stakeholders applying carbon farming practices. FiON has created a unified methodology to monitor and forecast  
47 agricultural carbon sequestration, by combining automated near real-time field measurements, weather data, satellite imagery,  
48 modeling and computing networks. In general, FiON follows the principles of other ecological observatory networks, such as  
49 National Ecological Observatory Network (NEON, Keller et al., 2008), Global Lake Ecological Observatory Network  
50 (GLEON, Hipsey et al., 2017) and Biodiversity Observatory Networks (GEOBON, Guerra et al., 2021) that collect long-term  
51 ecological data and monitor the effects of climate and land use change (Elmendorf 2016; Hinckley et al., 2016; Hipsey et al.,  
52 2017; Keller et al., 2008). The primary purpose of FiON, however, is to i) create new knowledge on soil processes, ii) to  
53 measure, verify and forecast the carbon sequestration in agricultural soils and to iii) approximate the effects of carbon farming  
54 practices on yield, biomass and CO<sub>2</sub> flux in near real-time. To achieve this, FiON invested in the use and development of a  
55 community cyberinfrastructure tool, Predictive Ecosystem Analyzer (PEcAn, pecanproject.org), which enables synthesizing  
56 different data sources and process-based models, quantifying and partitioning uncertainties, and operationalizing near real-  
57 time ecological forecasting (Fer et al., 2021). To disseminate the observations and findings, we built a free-access online  
58 dashboard called Field Observatory (v1.0, fieldobservatory.org). This website serves as a tool to monitor the impacts of carbon  
59 farming practices. The dashboard integrates data from field sensors, remote sensing and field survey. In this sense, FiON will  
60 provide decision support for the farmers, at first hand via the Field Observatory website and in due course via the scientific  
61 synthesis informed by the best available data and models. To serve the research and other interested communities, the data in  
62 Field Observatory is publicly available and downloadable from the website.

63

64 In this paper our objectives are to 1) describe data flows from various manual and automatic measurements in the Field  
65 observatory, 2) demonstrate 15-day forecasts of carbon exchange and plant growth towards decision support for the farmers,  
66 and 3) discuss the benefits of the public monitoring network established by FiON.

67

68 First, we introduce the sites included in FiON, and describe the tested carbon farming practices. Next, we describe the FiON  
69 workflow from data collection, processing and storage to visualization and dissemination through the Field Observatory  
70 website. Finally, we present the near real-time model-data synthesis, forecasting and decision support for the users.

## 71 **2 Sites and tested carbon farming practices**

72 The first phase of FiON consists of two intensive agricultural research sites and 20 voluntary farms testing carbon farming  
73 practices (Fig. 1, <https://www.fieldobservatory.org/MapView>). These 20 farms, called Advanced Carbon Action farms (ACA),  
74 were selected out of 100 pilot farms participating in the Carbon Action platform<sup>1</sup>, where volunteer farmers test carbon farming  
75 practices (Mattila et al. ~~2021~~2022). Each farm has a test field and an adjacent, conventionally managed, control field (field 1  
76 and 0 in Field Observatory, respectively). The additional carbon farming practices aim to increase carbon sequestrationstock  
77 through increasing carbon inputs (photosynthesis, ~~exogenous inputs~~ & soil amendments) or through decreasing carbon  
78 decomposition (Minasny et al., 2017). These practices (Table 1) are: cover crops, adaptive grazing, soil amendments,  
79 subsoiling and ley farming (introducing a grass crop into rotation). Each farmer made a five-year carbon farming plan and took  
80 soil samples at the beginning of the study from GPS located points in the field. The same points are monitored annually and  
81 also contain real-time soil sensors.

82

---

1

Carbon Action platform consists of several scientific projects, 100 farms committed to 5 years of research activity and farmer extension services. As of spring 2021, some 600 farmers are participating around the topic. Food system companies and organisations are also involved. Carbon Action is led by BSAG and the research is coordinated by FMI. More <https://carbonaction.org/en/front-page/>

83

84

**Table 1 Principles of the carbon farming practices tested at the Carbon Action farms.**

Carbon farming practice	Principles for carbon sequestration
Cover crops	Crops planted to lengthen photosynthetically active period and to increase carbon <del>assimilation,</del> <del>carbon inputs from above</del> and <del>root inputs</del> <u>belowground biomass</u> and to reduce leaching of carbon and nutrients.
Adaptive grazing	Short grazing & long rest periods to manage grass growth for increased root growth and increased soil cover.
Soil amendments	Exogenous carbon input. <del>In addition</del> <u>High input of organic material</u> may stimulate plant growth through increased water holding capacity, nutrients, etc.
Subsoiling	Removing physical barriers to root growth by soil loosening. Coupled to a grass crop to stabilize loosened soil. Increases plant growth and soil aeration and decreases bulk density.
Ley farming	Breaking monocropping with perennial grass. Increases photosynthesis, root input and diversity.
Grass cultivation	Diverse plant species composition, increased cutting height and organic fertilization.

85

86

87

88

89

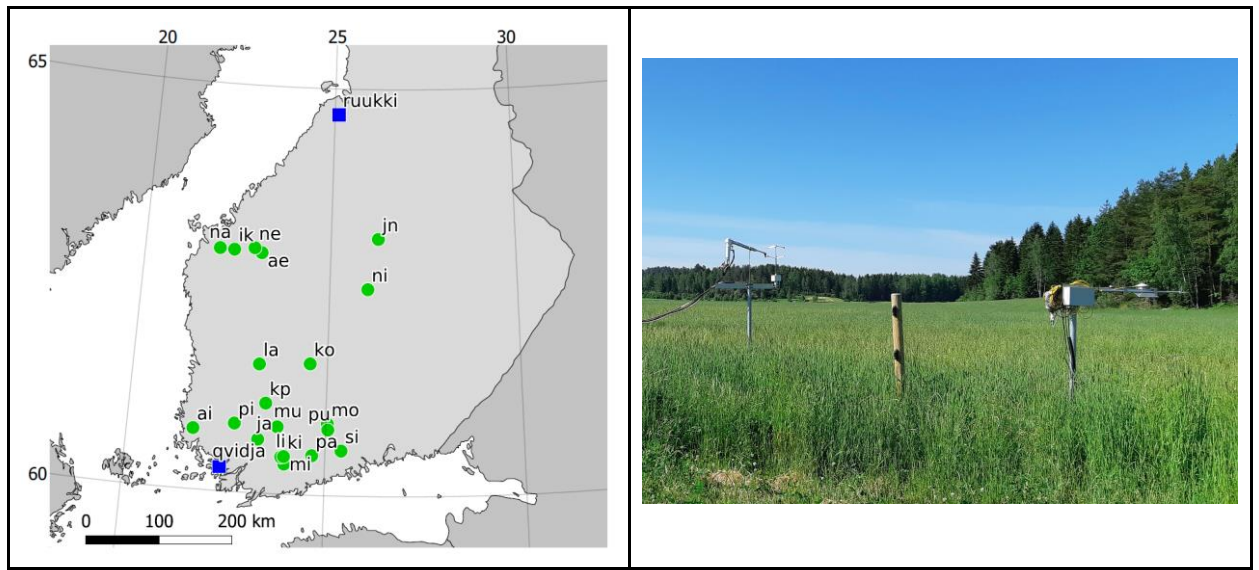
90

91

92

93

The 20 ACA farms were selected based on their chosen practice (four farms per measure), location (appropriate distances for survey work and even spread over Finnish farmland) and soil type (a mix of clay and sandy soils) (Table 2). All of them were included in a soil conditionquality survey in 2019 (Mattila, 2020). Farms with anomalous measurements or too large organic matter content or nutrient differences between the control and treatment plots in the initial phase of FiON were excluded from ACA farms. FiON includes two intensive research sites, Qvidja and ~~Ruuuki~~ Ruukki, which are operated by the Finnish Meteorological Institute (FMI). In Qvidja, carbon farming practices are tested in three different fields. In Ruukki, there are no carbon farming practices implemented at the moment. Both sites have eddy covariance towers which continuously monitor greenhouse gas fluxes and weather (see Sect. 3).



94

95 **Figure 1** Map of Advanced Carbon Action sites (green dots) and intensive sites (blue squares) (left), and eddy covariance  
 96 tower and radiation measurement instrumentation at Qvidja (right).

97

98 **Table 2** Current FiON sites.

Site	Site type	Soil type	Carbon farming practice	Species in 2020	Nearest FMI weather station
AE	ACA	Sandy loam	Subsoiling	Rye	Kauhava airport
KO	ACA	Silt	Subsoiling	Silage grass	Juupajoki Hyytiälä
KP	ACA	Clay loam	Subsoiling	Multi-species ley	Pirkkala airport
LA	ACA	Clay silt	Subsoiling	Oats	Pirkkala airport
JN	ACA	Fine sand	Adaptive grazing	Pasture grass	Vesanto Sonkari
MI	ACA	Clay loam	Adaptive grazing	Pasture grass	Lohja Porla
NI	ACA	Sand till	Adaptive grazing	Pasture grass	Jyväskylä airport AWOS
KI	ACA	Fine sand	Soil amendments	Multi-species ley	Somero Salkola
LI	ACA	Clay loam	Soil amendments	Spring wheat	Lohja Porla
PA	ACA	Clay loam	Soil amendments	Hay grass	Nurmijärvi Röykkä
PI	ACA	Clay loam	Soil amendments	Oats	Kaarina Yltöinen

MU	ACA	Clay loam	Grass mixture	Multi-species ley	Somero Salkola
NA	ACA	Loam	Cover crops	Peas	Vaasa airport
NE	ACA	Loam	Cover crops	Oats	Kauhava airport
PU	ACA	Silty clay loam	Cover crops	Oats	Mäntsälä Hirvihaara
SI	ACA	Clay loam	Cover crops	Multi-species ley	Porvoo Harabacka
AI	ACA	Silty clay	Ley farming	Multi-species ley	Rauma Pyynpää
JA	ACA	Clay loam	Ley farming	Multi-species ley	Jokioinen Ilmala
IK	ACA	Sand till	Ley farming	Silage grass	Seinäjäki Pelmaa
MO	ACA	Loam	Ley farming	Barley	Hämeenlinna Lammi Pappila
Qvidja	Intensive	Clay loam	Grass cultivation	Silage grass	Kaarina Yltöinen*
Ruukki	Intensive	Organic (peat)	-	Silage grass	Siikajoki Ruukki*

99 \*Intensive sites have their own micrometeorological measurements.

100  
101

### 3 Data collection

102 FiON combines multiple online and offline data streams with different temporal frequencies and geographical extent (Fig. 2,  
103 Table 3). These data streams flow into a server where the data are pre-processed (filtered, gap-filled, formatted) and model-  
104 data analyses are performed through an ecological cyberinfrastructure Predictive Ecosystem Analyzer (PEcAn, Fer et al.,  
105 2021). All observational and computational outputs are stored in the server and disseminated through a web-based user  
106 interface. In the following sections we describe each data stream and model-data activity in the order given in Fig. 2.

107

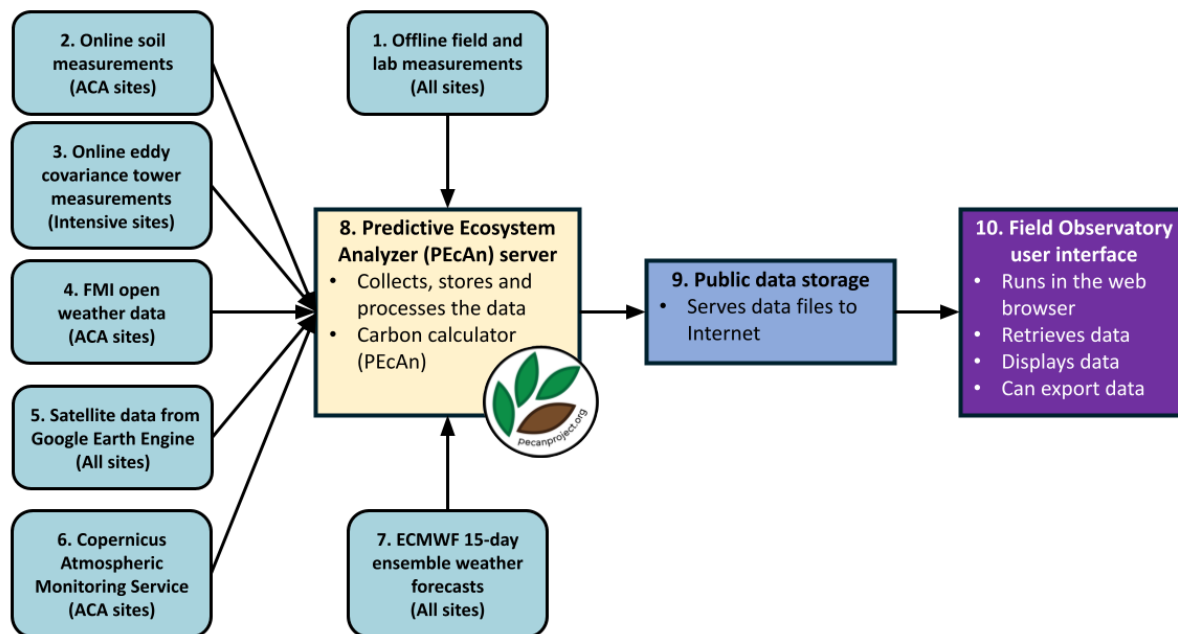


Figure 2 Overview of the FiON data flows.

### 3.1 Offline field and lab measurements

At ACA sites, the measurements are done at three, static measurement georeferenced points per field. The points have c.a. 30–100 m distance from each other and are located on a transect line. They were located to cover the variability of the The transect was situated on each field and cover similar soil to ensure comparable conditions infor both the test and control plots. When placing the transects, slope, vegetation map and soil type were used to ensure the transect covers different management zones in the field. Annual soil sampling and soil quality measurements are made within a ten-meter radius of these points. All offline data from ACA sites on soil properties (cation exchange capacity, pH, organic matter), nutrients (P, K, S, Ca, Mg, Cu, Zn, B, Mn, Fe, Al, P-saturation), soil physical quality (soil structure, bulk density, porosity, water holding capacity, infiltration rate) and biological properties (earthworm counts, above ground biomass, percentage plant cover) are presented in Zenodo data repository with annual updates (Mattila, 2020; Mattila and Heinonen, 2021). In addition to annual monitoring, a pre-study SOC sampling was conducted on the fields in 2018 and will be repeated in 2023. In these studies, ten 20 cm deep core soil samples (14 mm diameter) were collected at 10 m radius from a georeferenced point centre and pooled to form a composite sample. Such samples were taken from each field from the three measurement points from both the control and carbon farming fields. Focusing the sampling to georeferenced locations and using composite sampling, reduces the overall sampling

125 [variability and allows tracking relatively small \(4 % of background level\) changes in SOC stock \(Knebl et al. 2015\).](#) The  
126 offline field measurements at the intensive site Qvidja are described in Heimsch et al. (2021). [Such offline](#)  
127 [Offline](#), non-automated and infrequent data are currently being curated further for harmonization and reporting in JavaScript  
128 Object Notation (JSON) file formats and International Consortium for Agricultural Systems Applications (ICASA) standards  
129 (White et al., 2013). An example soil carbon measurement data point ( $16.59 \pm 2.25 \text{ kg m}^{-2}$ , average  $\pm$  standard deviation) is  
130 visualized on Qvidja graphs and available on the accompanying JSON file ([https://data.lit.fmi.fi/field-](https://data.lit.fmi.fi/field-observatory/qvidja/ec/events.json)  
131 [observatory/qvidja/ec/events.json](https://data.lit.fmi.fi/field-observatory/qvidja/ec/events.json)).

### 132 **3.1.1 Field activity**

133 All field activity information (e.g. planting, fertilization, harvest timing and amount) is currently received offline through  
134 personal communication. An online application is under development for i) harmonizing historical field data, and for ii)  
135 collecting future field activity data. Accordingly, the application is being developed to allow the farmers themselves to enter  
136 these events and related details, and it will be tested for the first time at the end of the 2021 season. The application is written  
137 using the Shiny R package (v1.6.0, Chang et al., 2021) and it automatically produces files in a JSON format using the ICASA  
138 standards when possible ([https://github.com/Ottis1/fo\\_management\\_data\\_input](https://github.com/Ottis1/fo_management_data_input)). Examples of historical field activity events  
139 (e.g. planting and tillage) that are prepared through this application are being made available in the Field Observatory JSON  
140 files and visualized on the graphs (Fig. 5).

### 141 **3.2 Online soil measurements**

142 Since 2020, each ACA site was provided with four TEROS-12 soil sensors (METER Group, Inc. USA) (two sensors per field,  
143 control and treatment) measuring volumetric water content, electrical conductivity and temperature (Table 3). The automated  
144 sensors are located at 75 mm depth in two of the three fixed measurement points of each field. The sensors were connected to  
145 a third party data transfer hardware (Datasense Oy, Finland), which uses Lora/WAN network to transmit the data. During the  
146 first year, the sensors measured every half hour but in 2021 measurement frequency was changed to one hour. The data is  
147 stored at the service providers server and is pulled to the PEcAn server (#8) through the Datasense API. Currently the sensor  
148 array includes 80 TEROS-12 soil sensors, four O<sub>2</sub> sensors (Apogee Instruments, [SO-120](#), USA) and two CO<sub>2</sub> sensors (Vaisala  
149 Oy, [G525](#), Finland) and will be supplemented with weather and groundwater depth measurements. [The soil O<sub>2</sub> and CO<sub>2</sub> meters](#)  
150 [are used to track changes in soil microbial activity and to guide model development.](#)

### 151 **3.3 Online eddy covariance ~~tower~~ measurements**

152 Carbon dioxide, evapotranspiration (latent heat), sensible heat and momentum fluxes between the ecosystem and atmosphere  
153 are measured at the intensive study sites, Ruukki and Qvidja, using the micrometeorological eddy covariance (EC) technique.  
154 The EC instrumentation at both sites includes a three-axis sonic anemometer (uSonic-2 Scientific, METEK GmbH, Elmshorn,



155 Germany) and an enclosed-path infrared gas analyser (LI-7200, LI-COR Biosciences, NE, USA) installed on a tower. The  
156 measurement height is 2.3 m in Qvidja and 3.3 m in Ruukki (2.3 m from 13 June to 25 June 2019 ~~and~~ 3.1 m from 25 June to  
157 4 November 2019 and 3.3 m since 5 November 2019). The measurement heights fulfill guidelines for grasslands and croplands  
158 defined by the Integrated Carbon Observation System (ICOS; Sabbatini & Papale, 2017). For details of the measurement set-  
159 up in Qvidja, see Heimsch et al. (2021).

160 The data from the EC instruments are recorded at a 10-Hz frequency. Half-hourly turbulent fluxes are calculated by block-  
161 averaging these raw data after applying a double rotation of the coordinate system (McMillen, 1988). The time lag between  
162 the sonic anemometer and gas analyzer signals is determined based on the cross-correlation analysis (Rebmann et al., 2012).  
163 The gas fluxes are calculated from the mixing ratios determined with respect to dry air (Webb et al., 1980). The measured  
164 fluxes are compensated for the losses due to high-frequency signal attenuation within the measurement system (Laurila et al.,  
165 2005). The flux data are filtered for instrument malfunction and unfavourable flow conditions according to the following  
166 generic validity criteria: number of spikes in the raw data < 100, mean CO<sub>2</sub> mixing ratio > 350 ppm, relative stationarity (Foken  
167 and Wichura, 1996) < 30 % and CO<sub>2</sub> mixing ratio variance < 15 ppm<sup>2</sup> from April to September and < 5 ppm<sup>2</sup> from October to  
168 March. At the Ruukki site, flux data are accepted from the wind direction sector 135°-315° (Blocks 5, 6, 5up and 6up) and the  
169 sectors 0°-90° and 330°-360° (Blocks 1-4). In Qvidja, the wind directions representing the direction of the experimental site  
170 are 0°-30° and 140°-360°. Periods of weak turbulence are filtered by applying a site-specific friction velocity threshold.  
171 The threshold and its uncertainty are estimated for each site-year using the moving-point-transition method (Reichstein et al.,  
172 2005) and a bootstrapping approach (Pastorello et al., 2020). For incomplete years, the estimates from the previous year are  
173 used. While the flux data provided online are screened, they will be subject to further quality control in offline post-processing  
174 that will produce the final datasets distributed for scientific use. These post-processing procedures include flux footprint  
175 analysis and related data screening for inadequate upwind fetch, i.e., for cases in which the measured flux does not  
176 predominantly represent the field. Footprints are calculated with respect to the effective measurement height that takes into  
177 account the varying canopy height and snow depth.

178 The EC measurements are complemented with supporting meteorological observations conducted next to the flux tower. These  
179 include soil moisture, soil temperature at different depths, soil heat flux, photosynthetically active radiation (PAR), global and  
180 reflected solar radiation, air temperature and precipitation. Half-hourly meteorological and flux data are transmitted to a server  
181 at the FMI, which is then synchronized to the PEcAn server (#8).

### 182 **3.3.1 Flux data processing, gap-filling and uncertainty analysis**

183 The missing CO<sub>2</sub> flux (net ecosystem exchange, NEE) data are gap-filled based on empirical response functions that are fitted  
184 separately for the gross primary production (GPP) and total ecosystem respiration (ER):

$$185 \quad NEE = GPP + ER \quad (1)$$

186 Respiration is modelled as a function of air temperature:

$$187 \quad ER = R_0 \cdot e^{E_0 \cdot \left( \frac{1}{T_0} - \frac{1}{T_a - T_1} \right)} \quad (2)$$

188 where  $R_0$  is the respiration rate at the reference temperature of 283.15 K,  $T_0 = 227.13$  K,  $T_1 = 56.02$  K,  $E_0$  is the temperature  
189 sensitivity of respiration, and  $T_a$  is the measured air temperature (Lloyd and Taylor, 1994).

190 GPP is modelled as a function of PAR:

$$191 \quad GPP = \frac{\alpha \cdot PAR \cdot GP_{max}}{\alpha \cdot PAR + GP_{max}} \quad (3)$$

192 where  $\alpha$  is the apparent quantum yield and  $GP_{max}$  is the asymptotic photosynthesis rate in optimal light conditions.

193 For gap-filling, the data are divided into bloek sections based on the harvest dates, and each bloek section is gap-filled  
194 separately. This is done because fluxes measured before a harvest cannot be used to predict fluxes after a harvest. First,  $R_0$  and  
195  $E_0$  are estimated from the night-time ( $PAR < 20 \mu\text{mol m}^{-2} \text{s}^{-1}$ ) flux data with a 15-day moving window. If there are less than  
196 25 observations, the window size is increased stepwise by two days until enough data are obtained. Similarly,  $\alpha$  and  $GP_{max}$  are  
197 determined with a three-day moving window by fitting the PAR response function to the daytime NEE from which the  
198 modelled respiration is subtracted. Finally, gaps in NEE are filled with modelled NEE, which is the sum of modelled GPP and  
199 modelled ER. Gap-filled values that are determined using fits from asymmetrical time windows, with possibly biased data are  
200 flagged and updated when new measurements become available. Before flux gap-filling, the missing air temperature and PAR  
201 data are imputed using linear interpolation if the gap is not longer than 6 h. Longer gaps are filled using the mean diel cycle of  
202 the data measured within seven days before or after the missing data point

203 The uncertainty of measured NEE ( $E_{meas}u_{meas}$ ) is inferred from the model residuals. For each site-year, the measurements are  
204 grouped into  $0.2 \text{ mg CO}_2 \text{ m}^{-2} \text{ s}^{-1}$  wide bins, and for each bin the measurement uncertainty is characterized as the standard  
205 deviation of the residuals. The uncertainty of each measured half-hourly flux is then estimated from the relation between the  
206 measurement uncertainty and the magnitude of the flux (Richardson et al., 2008). For incomplete years, the relation from the  
207 previous year is used.

208 The uncertainty of modelled NEE ( $E_{mod}u_{mod}$ , Eqs. (1)–(3)), is propagated from the uncertainties of the least-squares fits of  
209 modelled GPP ( $E_{GPP}u_{GPP}$ ) and Reco ( $E_{Reco}u_{Reco}$ ) as:

$$210 \quad E_{mod}u_{mod} = \sqrt{E_{GPP}^2 + E_{Reco}^2} = \sqrt{u_{GPP}^2 + u_{Reco}^2} \quad (4)$$

211

212 Finally, the uncertainty related to the friction velocity threshold ( $E_{ustarUustar}$ ) is estimated by filtering the flux data using the 100  
213 different bootstrapped friction velocity thresholds, gap-filling the 100 differently filtered datasets, and using the standard  
214 deviation of the gap-filled fluxes as an estimate for  $E_{ustarUustar}$ .

### 215 3.4 FMI open weather data

216 For all ACA sites, the weather information, namely precipitation, air temperature, relative humidity, wind speed and wind  
217 direction are retrieved from the nearest FMI weather stations (Table 2). Weather data are pulled to the PEcAn server using the  
218 fmir R package (<https://github.com/mikmart/fmir>).

### 219 3.5 Satellite data from Google Earth Engine (GEE)

220 All sites are monitored using remote sensing imagery from European Space Agency's (ESA) Sentinel-2 satellites.  
221 Atmospherically corrected Level-2A (L2A) Sentinel-2 multispectral data ([processed using Sen2Cor software](#)) are retrieved  
222 using GEE ([earthengine.google.com](http://earthengine.google.com)) cloud data platform. The scene classification band available in L2A products is used to  
223 filter away image acquisition dates during which the field is covered by snow, cloud or cloud shadow. [From the Sentinel-2](#)  
224 [data, we calculate the Normalized Difference Vegetation Index \(NDVI\) and the Leaf Area Index \(LAI\). LAI is calculated](#)  
225 [because it is present in and can be assimilated to many process-based ecosystem models. NDVI is included in Field](#)  
226 [Observatory mainly for the farmers to whom NDVI is a more familiar measure compared to LAI. NDVI is calculated using](#)  
227 near infra-red (B8A) and red (B4) bands of the L2A products. ~~The Leaf Area Index (LAI)~~ is estimated using the ESA Sentinel  
228 Application Platform (SNAP) Biophysical Processor neural network algorithm (Weiss & Baret, 2016,  
229 <https://github.com/onlinevalainen/satellitertools>). The NDVI data is natively available in 10 m resolution, whereas LAI is  
230 resampled to 10 m resolution from its original 20 m resolution. The satellite data is updated every two days at most (which is  
231 the Sentinel-2 revisit frequency over Finland). In addition, yearly cumulative NDVI sum is calculated using integration by  
232 trapezoidal rule for all sites ("NDVI days"). Common starting and ending points for the active growing season, 31 March and  
233 31 October, respectively, are used to standardize the cumulative NDVI sums between sites. [This standardization improves the](#)  
234 [comparability of the cumulative sums between sites by having them all in the same absolute units. Without standardization the](#)  
235 [cumulative sums would be much influenced by the availability of the first and last observations of the growing season for a](#)  
236 [site. This is determined more by the cloud cover than the actual start and end of the growing season.](#) To improve within site  
237 comparison, the cumulative NDVI is computed using dates when all fields within a site have satellite imagery available. The  
238 NDVI and LAI data is provided to the Field Observatory user interface in both raster (GeoTIFF) and tabular form (CSV).

239 With the tabular data, the average value of pixels within the field is used to estimate the field-level value. The tabular data is  
240 provided with 90 % confidence intervals by multiplying the associated uncertainties by ~~1.645~~ [the Z-score for two-sided 90 %](#)  
241 [confidence interval \(1.645\)](#). Non-realistic negative LAI values are capped to zero. For NDVI the uncertainty is presented as  
242 standard error of the mean (SE) of the pixels within the field. For the cumulative NDVI sum, the uncertainties are propagated

243 using the Python uncertainties package (<https://pythonhosted.org/uncertainties/>) which automatically computes the required  
244 derivatives and propagates the uncertainties.

245 The uncertainty for the LAI ( $u_{LAI}$ ) is estimated by combining the observational uncertainty ( $SE_{LAI}$ ) and the algorithmic  
246 uncertainty ( $u_{alg}$ ) of the LAI estimation:

$$247 \quad u_{LAI} = \sqrt{SE_{LAI}^2 + u_{alg}^2}, \quad (5)$$

248 where the  $SE_{LAI}$  is computed as the SE of LAI observations within the field. ~~The  $u_{alg}$  is calculated by propagating~~The  
249 observational uncertainty aims at capturing the uncertainty associated with a particular single observation (from a specific  
250 image at a certain date). It is affected by the variability of the individual pixel values within the field at that specific date. The  
251  $u_{alg}$  is calculated by propagating theoretical individual pixel uncertainties ( $u_{t_i}$ ) to the calculated average:

$$252 \quad u_{alg} = n^{-1} \sqrt{\sum_{i=1}^n u_{t_i}^2}, \quad (6)$$

253 where n is the number of pixels (i.e. sample size) and  $u_t$  the reported theoretical RMSE for the SNAP LAI algorithm that is  
254 0.89 (Weiss and Baret, 2016) and constant to all pixels. The artificial increase of n due to resampling LAI observations from  
255 its native 20 m resolution to 10 m is taken into account and n is reduced accordingly.

### 256 **3.6 PAR from Copernicus Atmospheric Monitoring Service (CAMS)**

257 For the ACA sites, the daily PAR data are derived from the global irradiation data obtained from the CAMS through daily  
258 queries ([www.soda-pro.com/web-services/radiation/cams-radiation-service/](http://www.soda-pro.com/web-services/radiation/cams-radiation-service/), Qu et al., 2017). The global daily irradiation (Wh  
259  $m^{-2} day^{-1}$ ) is converted to daily PAR ( $MJ m^{-2} day^{-1}$ ) assuming that 50 % of the global irradiation is at PAR range. The CAMS  
260 data is available for each day with a 48 h time lag. The daily PAR is reported in  $MJ m^{-2} day^{-1}$  which is a more convenient unit  
261 for a daily value compared to  $\mu mol m^{-2} s^{-1}$  used with 30-min measurement frequency in intensive sites.

### 262 **3.7 ECMWF 15-day ensemble weather forecasts**

263 European Center Medium-range Weather Forecast (ECMWF) data are processed by the Finnish Meteorological Institute for  
264 every site. This dataset consists of 6-hourly 2 meter temperature ( $2t$  variable in ECMWF standards), total precipitation ( $tp$ ),  
265 relative humidity ( $r$ ), 10 meter U and V wind components ( $10u$  and  $10v$ , respectively), surface pressure ( $sp$ ), surface solar and  
266 thermal radiation downwards ( $ssrd$  and  $strd$ , respectively) values of 51 ensemble members where one member is the control  
267 forecast and the other 50 are perturbed members which have perturbed initial conditions different than the control to explore

268 the range of uncertainty (Buizza and Richardson, 2017). Weather forecast data are updated everyday. Per ECMWF license  
 269 agreements, the data are visualized as is but the disseminated tabular files are obfuscated.

270 **Table 3 Summary of data streams reported in FiON. Offline = stored in public data repository and updated as necessary.**

Data type	Units	Data source	Frequency	Since	Sites	Online/offline
Field activity	-	Personal communication*	Seasonal	2019	All	Offline
Farmer management actions	-	Questionnaire	Annual		All	Offline
Soil C	% (ACA), kg m <sup>-2</sup> (Qvidja)	Lab measurements	Biannual	2018	All, except Ruukki	Offline
Soil water holding capacity	m <sup>3</sup> m <sup>-3</sup>	Lab measurements	Once to calibrate sensors	2019	All, except Ruukki	Offline
Soil nutrients	mg kg <sup>-1</sup>	Lab measurements	Biannual	2018	ACA	Offline
Bulk density	kg dm <sup>-3</sup>	Lab measurements	Annual	2019	ACA	Offline
Biomass	kg ha <sup>-1</sup>	Lab measurements	Annual	2019	ACA	Offline
Soil moisture	m <sup>3</sup> m <sup>-3</sup>	ACA soil sensors & eddy covariance	Half-hourly	2018 (Qvidja), 2019 (Ruukki), 2020 (ACA)	ACA & Intensive	Online
Soil temperature	°C	ACA soil sensors & eddy covariance	Half-hourly	2018 (Qvidja), 2019 (Ruukki), 2020 (ACA)	ACA & Intensive	Online
Electrical conductivity	μS cm <sup>-1</sup>	ACA soil sensors	Half-hourly	2020	ACA	Online
CO <sub>2</sub> -flux	mg m <sup>-2</sup> s <sup>-1</sup>	Eddy covariance	Half-hourly	2018 (Qvidja), 2019 (Ruukki)	Intensive	Online
Latent and sensible heat flux	W m <sup>-2</sup>	Eddy covariance	Half-hourly	2018 (Qvidja), 2019 (Ruukki)	Intensive	Online
Short-wave radiation (incoming and reflected)	W m <sup>-2</sup>	Eddy covariance	Half-hourly	2018 (Qvidja), 2019 (Ruukki)	Intensive	Online
CO <sub>2</sub> concentration	ppm	Eddy covariance	Half-hourly	2018 (Qvidja), 2019 (Ruukki)	Intensive	Online
Precipitation	mm	FMI open weather & eddy covariance	Half-hourly	2018 (Qvidja), 2019 (ACA & Ruukki)	ACA & Intensive	Online

Air Temperature	°C	FMI open weather & eddy covariance	Half-hourly	2018 (Qvidja), 2019 (ACA & Ruukki)	ACA & Intensive	Online
Relative Humidity	%	FMI open weather & eddy covariance	Half-hourly	2018 (Qvidja), 2019 (ACA & Ruukki)	ACA & Intensive	Online
PAR	MJ m <sup>-2</sup> day <sup>-1</sup> μmol m <sup>-2</sup> s <sup>-1</sup>	Copernicus & eddy covariance	Daily & half-hourly	2018 (Qvidja), 2019 (ACA & Ruukki)	ACA & Intensive	Online
Leaf Area Index	m <sup>2</sup> m <sup>-2</sup>	Sentinel-2, GEE	Min 2-days	2018 (Qvidja), 2019 (ACA & Ruukki)	All	Online
NDVI	-	Sentinel-2, GEE	Min 2-days	2018 (Qvidja), 2019 (ACA & Ruukki)	All	Online

271 \*Online application is under development.

### 272 3.8 Predictive Ecosystem Analyzer (PEcAn) server

273 All FiON data are pooled in an FMI server where model-data integration cyberinfrastructure software PEcAn is installed and  
274 compiled. PEcAn is an ecological informatics toolbox that consists of process-based models, a workflow management system  
275 and analytical tools for model-data synthesis (LeBauer et al., 2013; Dietze et al., 2013). The automated PEcAn workflow calls  
276 a series of modularized tasks that involve pre-processing of the model inputs, configuring and running the models, post-  
277 processing model outputs and performing model-data integration analyses. Coupling a process-based model to this workflow  
278 requires writing a model package which consists of a few interfacing scripts as PEcAn adopts intermediate input and output  
279 file formats, and applies pre- and post-model run analyses to these standards (Fer et al., 2021). While there are already many  
280 ecosystem models coupled to PEcAn and its design is general across process-based models, coupling of more models that can  
281 simulate agricultural ecosystems is in progress. In this study, we coupled the BASGRA\_N model (Basic Grassland Model,  
282 Höglind et al., 2020) to the PEcAn workflow and demonstrated its use for the Qvidja site (see Sect. 4, Model-data synthesis).  
283 In the future, we will provide model predictions for all sites through PEcAn.

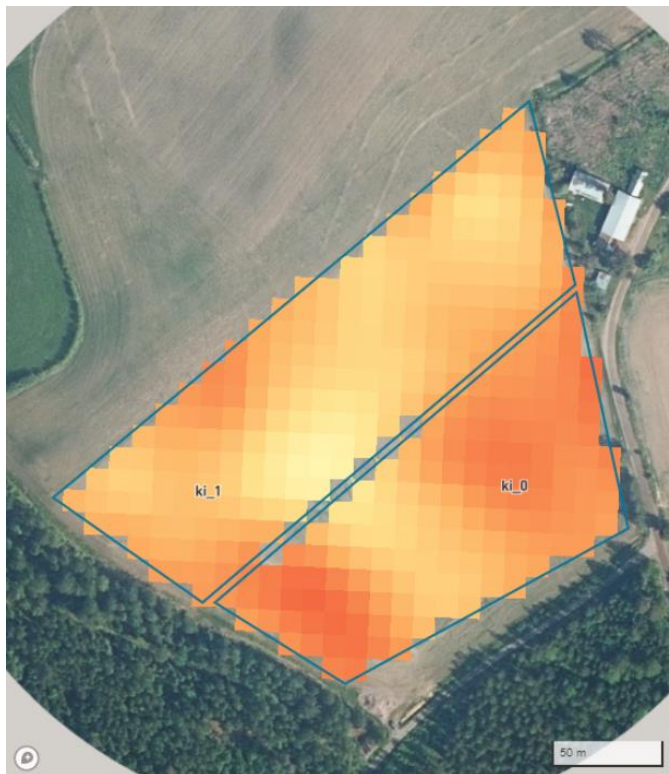
### 284 3.9 Public data storage

285 To harmonize the data, all tabular data with less than daily measurement frequency is aggregated to a 30 min interval (to every  
286 hour and half hour) before transferring the data to the public data storage (Amazon Simple Storage Service, field-  
287 observatory.data.lit.fmi.fi). To protect the privacy of the farmers, all data holding spatial information is transformed for all  
288 ACA sites, except for site MU (which is operated by Häme University of Applied Sciences).

289 **3.10 Field Observatory user interface**

290 The Field Observatory user interface (v1.0, fieldobservatory.org) allows viewing general information about the sites and the  
291 measurements and carbon farming practices conducted on them. The website has an interactive map to navigate to site-specific  
292 dashboards. A site view consists of general information about the site, an interactive map with satellite imagery of a specified  
293 vegetation parameter, an interactive timeline for selecting satellite imagery for viewing, and a panel of interactive time series  
294 charts (Fig. 3). Each chart comes with a description of the displayed data. A chart typically contains multiple time series and  
295 the visibility of each can be toggled. The user can enable and disable time aggregation and choose the time aggregation level  
296 from predefined options. The time aggregation is calculated using sliding statistics such as mean or sum depending on the data  
297 type. Any chart can be exported as an SVG image or as a CSV file containing the displayed data. A global specification file  
298 defines a list of charts and the data source types that can be shown in each chart. Site-specific specification files are used to  
299 define data source types available for each site and to provide links to the data files. Specification files are stored in JSON  
300 format.

301 The website is served by Azure services. The map and site views are based on client-side JavaScript, running in the user's web  
302 browser. Maps have been implemented using Mapbox GL JS JavaScript library.



**KI**

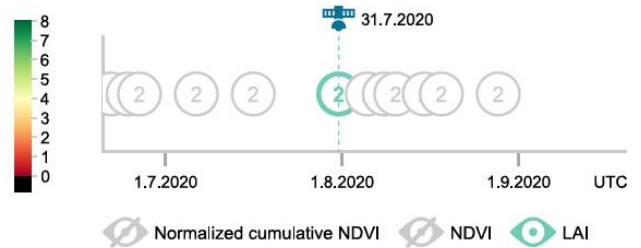
**Advanced CarbonAction Site**

KI field is a low OM sand in organic crop rotation. The aim is to increase OM by adding organic matter through soil amendments (wood pulp, ramial woodchips).

**FARMING METHODS**

Management: soil amendments  
Species: multi-species ley  
Soil type: fine sand

**SATELLITE IMAGES**

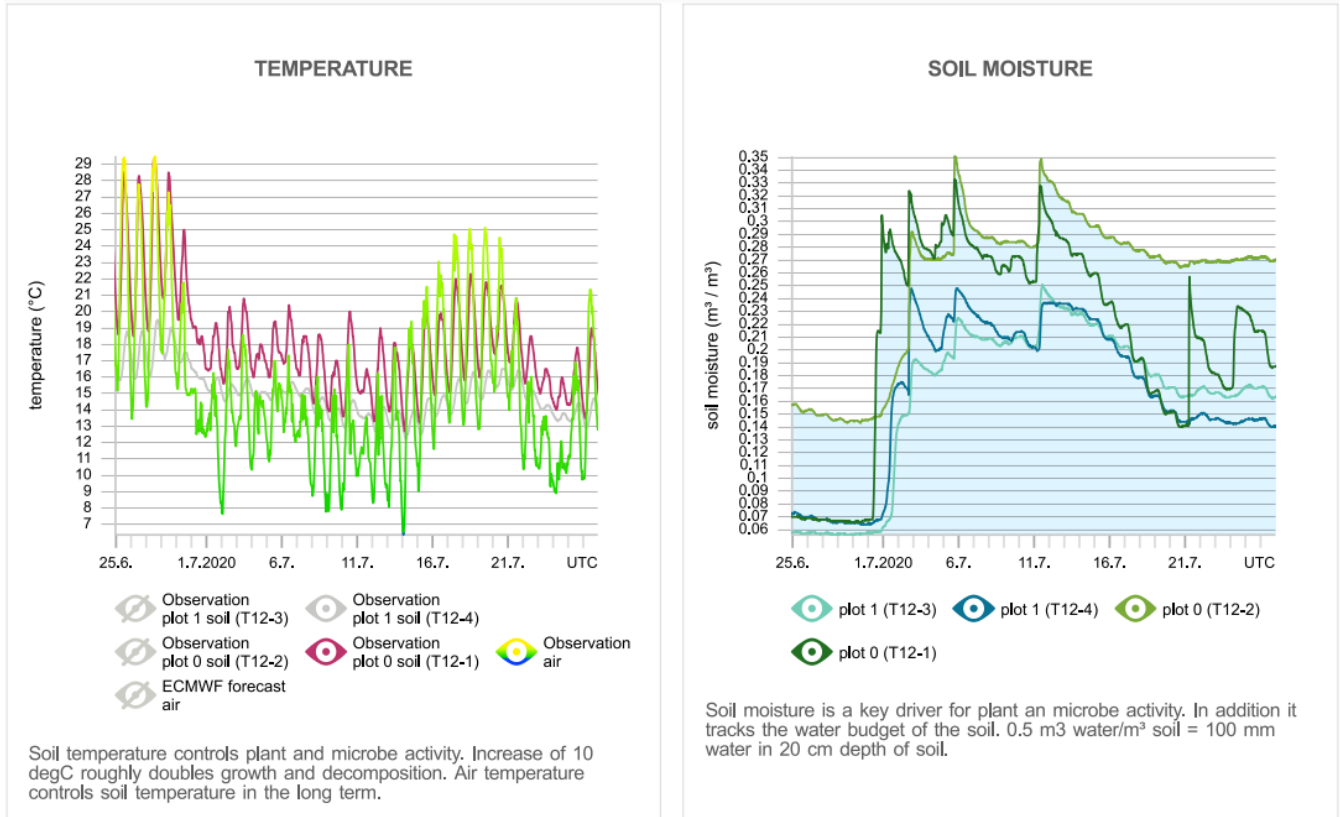


303

304 (a)

305

306



307

308

(b)

309 **Figure 3** Two web interface views of the measurement data for site KI: (a) Overview and LAI satellite images and (b) observed  
310 soil and air temperature and soil moisture. The reader is referred to the website [www.fieldobservatory.org](http://www.fieldobservatory.org) for more and  
311 interactive charts. The aerial photo contains data from the National Land Survey of Finland Topographic Database (11/2020).

#### 312 **4 Model-data synthesis and decision support**

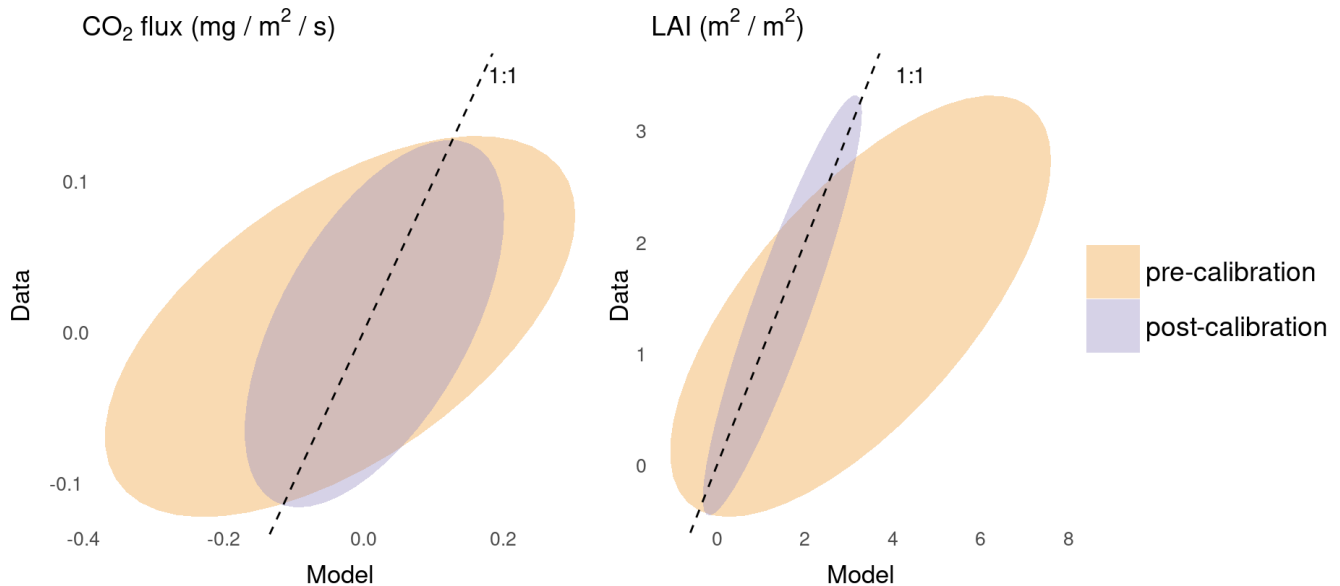
313 While the current version of the Field Observatory mainly disseminates observations, one of the main goals of this application  
314 is to provide accessible near real-time model-data synthesis, forecasting and decision support for the users. We demonstrate



315 the first application of this service at the Quidja grassland site with the grassland model BASGRA\_N (Table 2). BASGRA\_N  
316 model is developed specifically for northern climates and for grass types (timothy, *Phleum pratense*; meadow fescue, *Festuca*  
317 *pratensis*) that are the dominating forage species cultivated at the Quidja farm, and it is able to simulate grassland productivity,  
318 quality and greenhouse gas balance (Höglind et al., 2020).

319

320 We coupled BASGRA\_N to PEcAn, and used PEcAn's workflow management system and analytical tools (specifically the  
321 Bayesian calibration and state data assimilation modules) to inform the model with the data. Before employing them for  
322 forecasting and decision support, these models need to be initialized and calibrated. In other words, while state data assimilation  
323 algorithms can inform model states and improve predictive performance, best results are achieved when the model is calibrated  
324 to the site (Huang et al., 2021). Therefore, we used the field and lab measurements (Sect. 3.1), such as the rooting depth, soil  
325 carbon content and soil water holding capacity, to initialize the model states. Next, using multiple constraints (CO<sub>2</sub> flux and  
326 LAI from the eddy covariance tower field, Sect. 3.3), we calibrated 20 model parameters using Bayesian numerical methods  
327 through the BayesianTools R-package (Hartig et al., 2019) as implemented in the PEcAn system (Fer et al., 2018), also please  
328 see the supplement, section S1 for further details on the calibration protocol). In calibration, we used the observations from  
329 May 2018 to April 2021. After calibration model predictions were improved in terms of both uncertainty reduction and  
330 accuracy (Fig. 4). While the model is calibrated by the EC field data at Quidja, initial results show improvement at the nearby  
331 Quidja ACA sites as well (not shown here, but visible on Field Observatory LAI graphs).



332

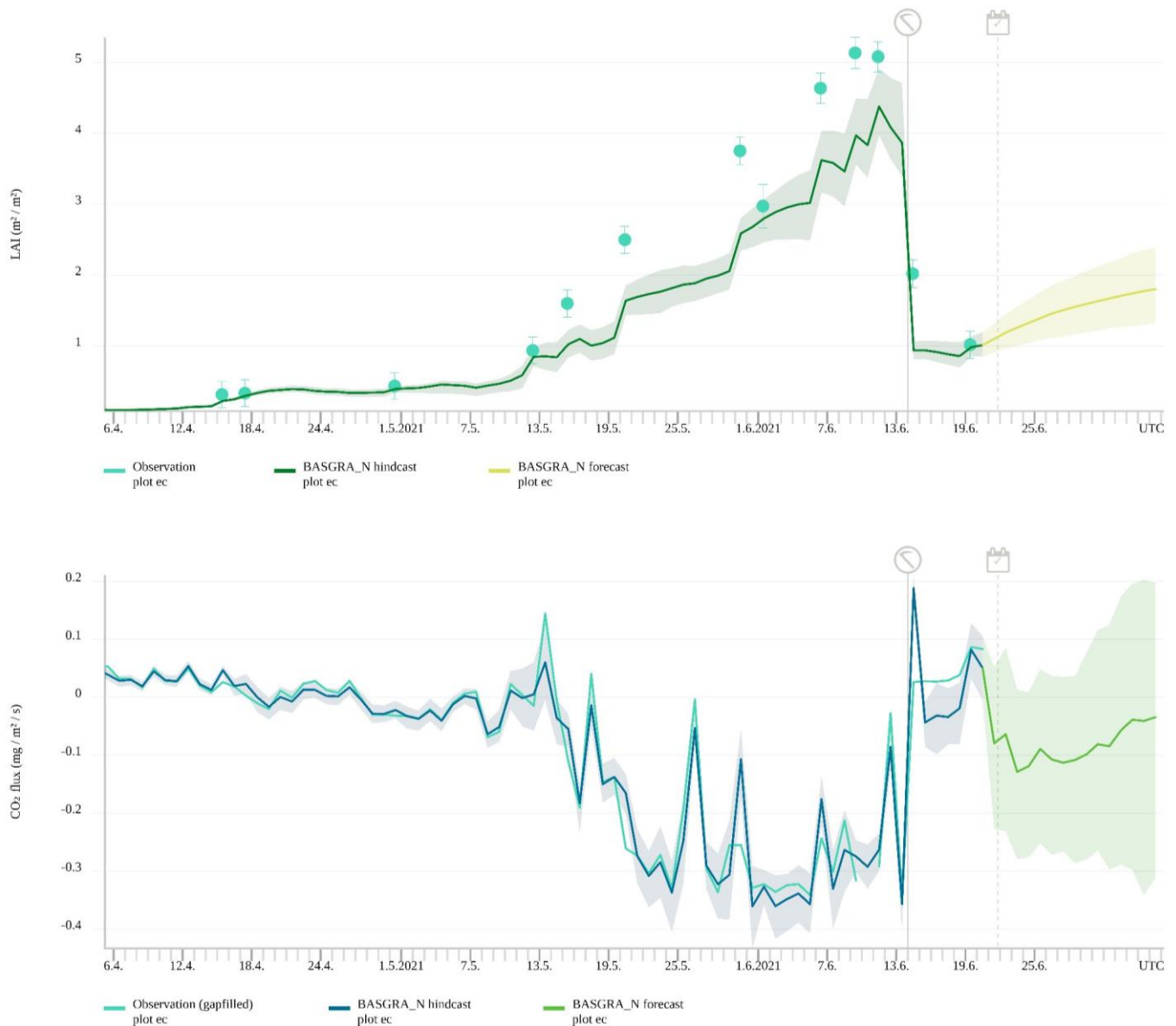
333

334 **Figure 4** Predicted versus observed comparison before (orange ellipses) and after (purple ellipses) initialization and  
335 calibration. Ellipses represent the 90% CI % confidence intervals of model ensemble runs with 500 members. After

336 initialization and calibration, the model performance at Quidja improved in terms of both accuracy (closer to the 1:1 line) and  
337 uncertainty reduction (narrower ellipses).

338

339 Next, we deployed the initialized and calibrated model in an online, operational, iterative near-term forecasting framework by  
340 driving it with the ECMWF ensemble 15-day weather forecast (Sect. 3.7). From April 2021 onwards, every day a 15-day  
341 ensemble forecast is made from the BASGRA\_N model. As time progresses, each day the CO<sub>2</sub> flux forecast is informed with  
342 the observed and gap-filled daily CO<sub>2</sub> flux values within an iterative forecast-analysis cycle using the ~~Extended~~ Ensemble  
343 Adjustment Kalman filter algorithm implemented in PEcAn (Dietze, 2017). When LAI observations are also available, they  
344 are jointly assimilated with the CO<sub>2</sub> flux measurements as well. Although we are currently only assimilating the CO<sub>2</sub> flux and  
345 LAI observations, related states are also updated within the model through the analysis step as the model encodes and simulates  
346 relations and covariances among different ecosystem processes. Among the model output variables, we share the LAI and CO<sub>2</sub>  
347 flux (Fig. 5), as well as Latent Heat and Yield Potential forecasts with the users through the Field Observatory user interface,  
348 albeit only for the Quidja site for the time being.



349

350 **Figure 5** 15-day LAI (top) and CO<sub>2</sub> flux (bottom) forecast at Qvidja. The 90 % confidence intervals for hindcast and forecast  
 351 are generated by 250 ensemble members, with different combinations of model parameters, initial conditions and  
 352 meteorological drivers. Units in the CO<sub>2</sub> flux graph are given per second to reflect the measurement frequency, however,  
 353 observations were aggregated to daily time step here to align with the model predictions. The scythe icon indicates a harvest  
 354 event on June 14th, 2021.

355

356 While a 15-day forecast has limited applicability within a cropping cycle, it could be informative on certain field activities that  
357 may have 1–2 weeks of flexibility which in return may have an impact on carbon balance. For instance, one can simulate  
358 alternative scenarios of timing of the harvest (e.g. whether to harvest now or delay it, please see supplementary material S2  
359 for a demonstration). It is possible to retrospectively explore these cases systematically as both weather forecasts and model  
360 analysis states are archived in the Field Observatory’s operational iterative forecasting system.

## 361 **5 Discussion**

362 This paper introduced the Field Observatory Network (FiON) and its unified methodology leading the way to monitor and  
363 forecast the functioning of agricultural ecosystems, geared towards verification of soil carbon sequestration. This methodology  
364 combines the existing spatially scattered measurements, modeling and computing networks, and disseminates the model-data  
365 computation outcomes through the Field Observatory user interface. In the following, we discuss the scientific and practical  
366 contributions of FiON and the Field Observatory, and the future steps planned for both.

### 367 **5.1 Scientific contribution**

368 FiON adopts state-of-the-art field and laboratory methods, open data sources, near real-time satellite imagery processing and  
369 model-data integration cyberinfrastructures—all of which are needed for a reliable MRV platform. A distinct feature of FiON  
370 is the network of ordinary farms, ACA sites, to establish baseline trends and verify additional changes. As soil carbon pool  
371 changes slowly, even after a shift in management practices, long-term monitoring is needed. The ACA sites (with control and  
372 treatment plots) were specifically designed for this purpose and will be monitored continuously for at least the next five years,  
373 and FiON aspires to continue even longer. This is an adequate time frame to detect SOC changes because the fastest carbon  
374 re-accumulation occurs in the first 10–20 years, depending on soil type, management practices, climate and initial SOC (Bossio  
375 et al., 2020), all of which are monitored by FiON. The intensive and ACA sites provide an important benchmarking opportunity  
376 to our model-data synthesis methodology which will be applied to all 100 Carbon Action farms.

377  
378 The PEcAn platform is central to our methodology; it enables synthesizing different data sources and process-based models,  
379 managing observational and model uncertainties, and near real-time forecasting. It distinguishes FiON from observations-only  
380 approaches. In addition to potentially having practical relevance for improving carbon storage, near-term agricultural  
381 forecasting has benefits to basic carbon science. Data assimilation methods help dissect model behaviour and identify research  
382 needs (Viskari et al., 2020). For instance, variability patterns of the best parameter sets in time and space can be identified by  
383 studying model ensemble members with respect to the analysis states (i.e. our best understanding about the system) and may  
384 point to unaccounted processes in models and underlying sources driving variability. If we manage to account for these  
385 variabilities (e.g. adding covariates that explain temporal variability), we could also improve our capability to model the carbon  
386 sequestration on the long term. Moreover, near-term iterative forecasting provides an out-of-sample way of statistical testing

387 for models which is less prone to overfitting than in-sample tests which are more typical in (agro-)ecology where models are  
388 tested against data that has already been observed (Dietze et al., 2018). Accordingly, a more in-depth analysis of the archived  
389 Field Observatory forecasting results and skills are ongoing and will be reported in a future study. In addition to understanding  
390 models better, operational iterative near-term forecasting also allows us to detect and intervene when measurements of certain  
391 sensors or data streams deviate from the assimilated background, and in return supports the management of the sensors and  
392 data pipelines, resulting in higher quality datasets. Overall, our 15-day iterative forecasting system provides continuous  
393 quantitative benchmarking of models and data based on all other available information, which allows rapid detection and  
394 explanation of changing patterns in the carbon sequestration with the possibility of intervening and making adjustments.

## 395 **5.2 Practical contribution**

396 The Field Observatory user interface has not only enabled farmers to monitor impacts of their carbon farming practices, but  
397 also to connect and compare their own and others' data and practices. Features in the user interface are co-created with the  
398 farmers and developed accordingly. For example, farmers requested to see a cumulative sum of NDVI through the growing  
399 season which was in return calculated and included on the website. Likewise, simple and clear descriptions to interpret each  
400 data type have been found helpful. The gap-filled CO<sub>2</sub> fluxes at the intensive study sites have made it easier to communicate  
401 carbon exchanges between land and the atmosphere and how carbon budget calculations are done. As a result, the Field  
402 Observatory has already been used in workshops and meetings with stakeholders, and in training and scientific outreach for  
403 the Carbon Action farmers.

404  
405 One of our aims with this framework is to provide decision support for the end users. This is effectively offered by Field  
406 Observatory in terms of feedback where end users can monitor the impact of their activities in a quantitative manner, assess  
407 and make their decisions in the future accordingly. Our framework also lays the groundwork for a more explicit and specific  
408 decision support system. Although such functionality is not fully in place yet (but ~~planned for the future versions~~under  
409 development), establishing the operational data assimilation and iterative forecasting pipeline is a milestone towards this  
410 direction. ~~Users~~While the 15 days' horizon has limitations with respect to the span of a production cycle, in the future we are  
411 planning to include seasonal, annual and longer term forecasts as well. However, 15-day forecasts can still provide decision  
412 support for relatively shorter term and flexible agricultural actions (such as harvest, irrigation, grazing etc.). With the additional  
413 layer of agricultural forecast on top of the weather forecasting services, users are quantitatively informed about the progression  
414 of various ecosystem states and services ~~by~~through these Field Observatory near-term forecast updates. ~~The~~For example,  
415 sensor or model-based dynamic fertilization strategies have successfully improved the nitrogen use efficiency of cropping  
416 systems (e.g. Sela et al., 2018; Scharf et al., 2011). Likewise, timing of harvest and the cutting height may affect the overall  
417 carbon budget and economic income, and the plants' water demand may necessitate a different irrigation scheme for optimum  
418 growth and water usage, all of which may not readily manifest themselves through weather forecasts and observations only.

419 We also acknowledge that such interventions are potentially easier for grasslands, as opposed to the croplands. Nevertheless,  
420 our operative iterative near-term forecasting system enables a framework to explore the impacts of such interventions  
421 dynamically, systematically and quantitatively, and in return devise more reliable and comprehensive decision criteria. Overall,  
422 the current pipeline is ~~further~~ being developed to improve the model performance and to be put into an adaptive decision  
423 making framework where alternative scenarios will be simulated with the ~~model~~models to aid users in their day-to-day  
424 operations ~~specific to their management structure and goals~~.

425  
426 The near-term carbon forecasts have also improved our communication with stakeholders in general. Reporting quantitative,  
427 specific and iterative carbon forecasts makes it possible to convey the idea that predictive carbon science has the potential to  
428 be as successful and common as numerical weather prediction (NWP) as a discipline and as a service to society one day.  
429 Ecological forecasts provide us with a standard, quantitative, intuitive and management-relevant method and language to  
430 develop the right context and tools for structuring soil carbon sequestration decisions (Petchey et al., 2015; Dietze et al., 2018).  
431 Bringing near-term carbon forecasts forward further helps describe that soil carbon monitoring and modeling is a complex  
432 computational problem that depends on vast amounts of basic scientific research and observations. It involves a diverse range  
433 of actors and organizations and requires efficient communication and continuous transfer of knowledge between these groups,  
434 similar to NWP (Bauer et al., 2015). Not only the similarities but also the differences between agricultural forecasting and  
435 NWP help clarify and re-focus the research needs (e.g. the need to address the heterogeneity and inherent variability in carbon  
436 systems). Overall, near-term forecasts help establish this constructive dynamic between researchers and stakeholders which in  
437 return helps tackle remaining bottlenecks for improving soil carbon sequestration more efficiently.

438  
439 There is a large interest towards adopting and developing Field Observatory further. Therefore, the website is under constant  
440 development with new features, and new information about carbon farming and findings of FiON are increasingly being made  
441 available.

### 442 **5.3 Avenues for future research and development**

443 We have planned future steps for both FiON and the Field Observatory. The first step is to add more agricultural models to  
444 PEcAn. This enables us to extend model-data analysis to all FiON sites where different species and management practices are  
445 involved (i.e. other than grass harvest timing and amount). Coupling of one such additional model (Simulateur  
446 multIdisciplinaire pour les Cultures Standard, STICS, Brisson et al., 1998) to PEcAn has already been completed, and others  
447 are in progress. In the meantime, more sites will be added to FiON, not only in number but also in type. For example, with  
448 carbon-smart planning, urban vegetation also has potential to store more carbon. We study this also in FiON and consequently  
449 urban sites will be added. Another goal is to include forests and peatlands in FiON, which requires incorporating new process-  
450 based models in the FiON workflow. During the coming years, more field and laboratory measurement data will be collected  
451 and used to validate the model estimates and re-calibrate the models.

452

453 The framework designed by FiON and described in this paper provides the necessary mechanics to study the applicability and  
454 reliability of the models to simulate components of the carbon budget virtually in every field. While scalability has been the  
455 core idea for the design of this framework since the beginning, putting it to practical test is the main scientific next step.  
456 Currently, a factorial experimental design and simulation is ongoing where the performance of the models will be tested at  
457 multiple sites by informing them with various data streams. For this, we will start with constraints that can be made available  
458 virtually from everywhere and test which combinations, if any, can inform models enough to capture local carbon budget  
459 dynamics and components. Such constraints are for example LAI derived from remote sensing, soil moisture provided by  
460 inexpensive in-situ sensors, soil properties estimated from global products and yield. In this setup, the information contributed  
461 by the sites that are equipped with EC-towers will also be tested. For example, we will perform a factorial experiment at the  
462 ACA sites with and without the models being constrained by EC-data at the intensive sites. As we have additional data streams  
463 other than the mentioned constraint data types (e.g. biomass and soil C, Table 2) from ACA sites for evaluation, the framework  
464 described in this paper provides the means to carry out such multi-site in-depth analyses.

465

466 The development of the online application to gather field activity data from farmers is also in progress. ~~This~~The main purpose  
467 of this application will not only allow us to make collection and utilization of field activity data in visualization and  
468 model-data synthesis but it will also pipelines easy. In this context, Field Observatory’s interoperability with commercial farm  
469 management information systems needs to be studied in order to reduce the number of times farmers are filling out such  
470 information. An additional future use of this online application is planned to enable the farmers to simulate a predefined  
471 number of scenarios regarding their day-to-day operations by triggering automated PEcAn workflows—for example, given  
472 the next 15-day forecast, they will be able to optimize the timing and amounts of their field activity. ~~In~~We are also considering  
473 utilizing this context, Field Observatory’s interoperability with commercial farm management online application for additional  
474 purposes: a) for compiling information systems needs from farmers regarding the flexibilities of their activities as this brings  
475 an additional practical constraint on the development of the model-based decision support system, b) for enabling new users  
476 to submit electronic requests and information about their fields to be studied, part of the FiON network, c) for supporting peer-  
477 to-peer learning between farmers (Mattila et al., 2022).

478

479 We are currently also investigating the use of satellite data sources other than Sentinel-2 in retrieving information on vegetation  
480 and soil properties. In addition to satellite imagery, drones could be used as a source of remote sensing data. The current  
481 Sentinel-2 data filtering is based on the cloud detection available in the L2A products. This filtering approach has produced  
482 quite clean time series; some sites do not have any outliers and some have at the maximum one or two per year. The benefit  
483 of our methodology—where we assimilate observations as state variables to process-based models—is that single outliers,  
484 with optimally larger uncertainties, do not have too drastic of an effect on the model predictions. Nevertheless, we will continue

485 [to follow the performance of the filtering approach and improve it if necessary.](#) Finally, the data streams used in data  
486 assimilation (to inform and update forecasts) will be increased and improvement in forecasting skills will be analyzed.

## 487 **6 Conclusions**

488 The Field Observatory Network (FiON) introduced in this paper is primarily a network of researchers, farmers, companies and  
489 other stakeholders developing carbon farming practices. FiON provides a unified methodology to monitor and forecast  
490 agricultural carbon sequestration by combining offline and near real-time field measurements, weather data, satellite imagery,  
491 modeling and computing networks. FiON disseminates data through the Field Observatory user interface  
492 ([www.fieldobservatory.org](http://www.fieldobservatory.org)). For farmers, FiON serves as a monitoring and decision support tool. In contrast to the mainstream  
493 decision support tools, FiON also provides the farmers access to other carbon farmers' data in the network. This enables  
494 comparisons and knowledge transfer between the carbon farmers.

495 FiON has several analogies to other ecological observatory networks, but unlike these existing networks, FiON is designed to  
496 provide near real-time information and forecasts concerning the carbon farming practices and to facilitate monitoring and  
497 verification of carbon sequestration. In this sense, FiON takes several steps forward from the mainstream of the ecological  
498 observatory networks known so far.

## 499 **7 Data availability**

500 The data displayed in the Field Observatory are available from the Field Observatory website ([www.fieldobservatory.org](http://www.fieldobservatory.org)) and  
501 from Amazon Simple Storage Service at <https://field-observatory.data.lit.fmi.fi/index.html>. Field measurements conducted at  
502 ACA sites in 2019 and 2020 are available from Zenodo data repository (Mattila, 2020; Mattila and Heinonen, 2021).

## 503 **8 Code availability**

504 The satellite data processing codes are available from a public GitHub repository  
505 (<https://github.com/onlinevalainen/satellitertools>). All PEcAn code is available openly on a GitHub repository  
506 (<https://github.com/PecanProject/pecan>). Field Activity data collection and curation application code which is under  
507 development is also available via GitHub ([https://github.com/Ottis1/fo\\_management\\_data\\_input](https://github.com/Ottis1/fo_management_data_input)). Rest of the codes by the  
508 authors are not yet openly available.

509



510 **9 Author contribution**

511 Conceptualization, ON, ONi, IF, AJ, TM, OK, JK, LH, LM, PJ, LK, ÅS, AL, JHe, IK, JL; Data curation, ON, IF, ONi, TM,  
512 OKu; Formal Analysis, ON, IF, ONi, TM, LHe, HV, SG, TV, JV, JT, Funding acquisition, TM, LK, AL, TL, JHe, TA, IK, JL;  
513 Investigation, ON, IF, ONi, TM, LHe, HV, SG, TV, JV, JT; Methodology, ON, IF, ONi, TM, HV, LK, OKu, TV, JV, JT, JHe,  
514 TA, JL; Project administration, TM, JK, LH, LK, ÅS, AL, TL, JHe, TA, IK, JL; Software, ON, ONi, IF, AJ, OK, OKu, HV,  
515 TV, JV, JT; Visualization, ON, ONi, IF, AJ, LM, PJ, OKu and comments from all; Writing – original draft preparation, all  
516 authors; Writing – review & editing, all authors.

517 **10 Competing interests**

518 The authors declare that they have no conflict of interest.

519 **11 Acknowledgments**

520 The work of HAMK has been conducted within the research project: *Carbon 4.0 - Analysis and utilization of biological data*  
521 *in complex carbon ecosystems* funded by the Ministry of Education and Culture (of Finland). [grant OKM/189/523/2018]. The  
522 work by FMI was supported by Business Finland [grant 6905/31/2018], The Strategic Research Council at the Academy of  
523 Finland [decision no 327214], the Academy of Finland Flagship Program [decision no 337552], the Ministry of Agriculture  
524 and Forestry of Finland [grant VN/5094/2021] and Maj and Tor Nessling foundation (grant 202000391). The work by SYKE  
525 was supported by The Strategic Research Council at the Academy of Finland [decision no 327350].

526

527 The authors want to thank the 20 farmers who allowed testing the framework on their Carbon Action fields. We also thank the  
528 owner of Ruukki farm, Natural Resources Institute Finland (Luke), and their employees for making it possible to have a  
529 measurement site there. In addition, we are thankful for the owners and staff of Qvidja farm.

530 **References**

531 [Bauer, P., Thorpe, A., and Brunet, G.: The quiet revolution of numerical weather prediction, Nature, 525, 47–55,](https://doi.org/10.1038/nature14956)  
532 [https://doi.org/10.1038/nature14956, 2015.](https://doi.org/10.1038/nature14956)

533 Bellamy, P. H., Loveland, P. J., Bradley, R. I., Lark, R. M., and Kirk, G. J. D.: Carbon losses from all soils across England  
534 and Wales 1978–2003, Nature, 437, 245–248, <https://doi.org/10.1038/nature04038>, 2005.

- 535 Bossio, D. A., Cook-Patton, S. C., Ellis, P. W., Fargione, J., Sanderman, J., Smith, P., Wood, S., Zomer, R. J., von Unger, M.,  
536 Emmer, I. M., and Griscom, B. W.: The role of soil carbon in natural climate solutions, *Nat Sustain*, 3, 391–398,  
537 <https://doi.org/10.1038/s41893-020-0491-z>, 2020.
- 538 Buizza, R. and Richardson, D.: 25 years of ensemble forecasting at ECMWF, <https://doi.org/10.21957/BV418O>, 2017.
- 539 Chang, W., Cheng, J., Allaire, J., Xie, Y., and McPherson, J.: Shiny: web application framework for R, 1, 2017, 2017.
- 540 Crowther, T. W., van den Hoogen, J., Wan, J., Mayes, M. A., Keiser, A. D., Mo, L., Averill, C., and Maynard, D. S.: The  
541 global soil community and its influence on biogeochemistry, *Science*, 365, eaav0550, <https://doi.org/10.1126/science.aav0550>,  
542 2019.
- 543 Dietze, M.: *Ecological Forecasting*, Princeton University Press, <https://doi.org/10.1515/9781400885459>, 2017.
- 544 [Dietze, M. C., Fox, A., Beck-Johnson, L. M., Betancourt, J. L., Hooten, M. B., Jarnevich, C. S., Keitt, T. H., Kenney, M. A.,](#)  
545 [Laney, C. M., Larsen, L. G., Loeschner, H. W., Lunch, C. K., Pijanowski, B. C., Randerson, J. T., Read, E. K., Tredennick, A.](#)  
546 [T., Vargas, R., Weathers, K. C., and White, E. P.: Iterative near-term ecological forecasting: Needs, opportunities, and](#)  
547 [challenges, \*Proc Natl Acad Sci USA\*, 115, 1424–1432, <https://doi.org/10.1073/pnas.1710231115>, 2018.](#)
- 548 Elmendorf, S. C., Jones, K. D., Cook, B. I., Diez, J. M., Enquist, C. A. F., Hufft, R. A., Jones, M. O., Mazer, S. J., Miller-  
549 Rushing, A. J., Moore, D. J. P., Schwartz, M. D., and Weltzin, J. F.: The plant phenology monitoring design for The National  
550 Ecological Observatory Network, *Ecosphere*, 7, e01303, <https://doi.org/10.1002/ecs2.1303>, 2016.
- 551 Fer, I., Kelly, R., Moorcroft, P. R., Richardson, A. D., Cowdery, E. M., and Dietze, M. C.: Linking big models to big data:  
552 efficient ecosystem model calibration through Bayesian model emulation, *Biogeosciences*, 15, 5801–5830,  
553 <https://doi.org/10.5194/bg-15-5801-2018>, 2018.
- 554 Fer, I., Gardella, A. K., Shiklomanov, A. N., Campbell, E. E., Cowdery, E. M., De Kauwe, M. G., Desai, A., Duveneck, M. J.,  
555 Fisher, J. B., Haynes, K. D., Hoffman, F. M., Johnston, M. R., Kooper, R., LeBauer, D. S., Mantooth, J., Parton, W. J., Poulter,  
556 B., Quaipe, T., Raiho, A., Schaefer, K., Serbin, S. P., Simkins, J., Wilcox, K. R., Viskari, T., and Dietze, M. C.: Beyond  
557 ecosystem modeling: A roadmap to community cyberinfrastructure for ecological data-model integration, *Glob. Change Biol.*,  
558 27, 13–26, <https://doi.org/10.1111/gcb.15409>, 2021.
- 559 Foken, Th. and Wichura, B.: Tools for quality assessment of surface-based flux measurements, *Agricultural and Forest*  
560 *Meteorology*, 78, 83–105, [https://doi.org/10.1016/0168-1923\(95\)02248-1](https://doi.org/10.1016/0168-1923(95)02248-1), 1996.
- 561 Guerra, C. A., Bardgett, R. D., Caon, L., Crowther, T. W., Delgado-Baquerizo, M., Montanarella, L., Navarro, L. M., Orgiazzi,  
562 A., Singh, B. K., Tedersoo, L., Vargas-Rojas, R., Briones, M. J. I., Buscot, F., Cameron, E. K., Cesarz, S., Chatzinotas, A.,  
563 Cowan, D. A., Djukic, I., van den Hoogen, J., Lehmann, A., Maestre, F. T., Marín, C., Reitz, T., Rillig, M. C., Smith, L. C.,

- 564 de Vries, F. T., Weigelt, A., Wall, D. H., and Eisenhauer, N.: Tracking, targeting, and conserving soil biodiversity, *Science*,  
565 371, 239–241, <https://doi.org/10.1126/science.abd7926>, 2021.
- 566 Heikkinen, J., Ketoja, E., Nuutinen, V., and Regina, K.: Declining trend of carbon in Finnish cropland soils in 1974–2009,  
567 *Glob Change Biol*, 19, 1456–1469, <https://doi.org/10.1111/gcb.12137>, 2013.
- 568 Heikkinen, J., Keskinen, R., Regina, K., Honkanen, H., and Nuutinen, V.: Estimation of carbon stocks in boreal cropland soils  
569 - methodological considerations, *Eur J Soil Sci*, 72, 934–945, <https://doi.org/10.1111/ejss.13033>, 2021.
- 570 Heimsch, L., Lohila, A., Tuovinen, J.-P., Vekuri, H., Heinonsalo, J., Nevalainen, O., Korhonen, M., Liski, J., Laurila, T.,  
571 and Kulmala, L.: Carbon dioxide fluxes and carbon balance of an agricultural grassland in southern Finland, *Biogeosciences*,  
572 18, 3467–3483, <https://doi.org/10.5194/bg-18-3467-2021>, 2021.
- 573 Hinckley, E. S., Bonan, G. B., Bowen, G. J., Colman, B. P., Duffy, P. A., Goodale, C. L., Houlton, B. Z., Marín-Spiotta, E.,  
574 Ogle, K., Ollinger, S. V., Paul, E. A., Vitousek, P. M., Weathers, K. C., and Williams, D. G.: The soil and plant biogeochemistry  
575 sampling design for The National Ecological Observatory Network, *Ecosphere*, 7, <https://doi.org/10.1002/ecs2.1234>, 2016.
- 576 Hipsey, M. R., Bruce, L. C., Boon, C., Busch, B., Carey, C. C., Hamilton, D. P., Hanson, P. C., Read, J. S., de Sousa, E.,  
577 Weber, M., and Winslow, L. A.: A General Lake Model (GLM 3.0) for linking with high-frequency sensor data from the  
578 Global Lake Ecological Observatory Network (GLEON), *Geosci. Model Dev.*, 12, 473–523, [https://doi.org/10.5194/gmd-12-](https://doi.org/10.5194/gmd-12-473-2019)  
579 [473-2019](https://doi.org/10.5194/gmd-12-473-2019), 2019.
- 580 Höglind, M., Cameron, D., Persson, T., Huang, X., and van Oijen, M.: BASGRA\_N: A model for grassland productivity,  
581 quality and greenhouse gas balance, *Ecological Modelling*, 417, 108925, <https://doi.org/10.1016/j.ecolmodel.2019.108925>,  
582 2020.
- 583 [Huang, X., Zhao, G., Zorn, C., Tao, F., Ni, S., Zhang, W., Tu, T., and Höglind, M.: Grass modelling in data-limited areas by](https://doi.org/10.1016/j.fcr.2021.108250)  
584 [incorporating MODIS data products, \*Field Crops Research\*, 271, 108250, <https://doi.org/10.1016/j.fcr.2021.108250>, 2021.](https://doi.org/10.1016/j.fcr.2021.108250)
- 585 Keller, M., Schimel, D. S., Hargrove, W. W., and Hoffman, F. M.: A continental strategy for the National Ecological  
586 Observatory Network, *Frontiers in Ecology and the Environment*, 6, 282–284, [https://doi.org/10.1890/1540-](https://doi.org/10.1890/1540-9295(2008)6[282:ACSFTN]2.0.CO;2)  
587 [9295\(2008\)6\[282:ACSFTN\]2.0.CO;2](https://doi.org/10.1890/1540-9295(2008)6[282:ACSFTN]2.0.CO;2), 2008.
- 588 [Knebl, L., Leithold, G., and Brock, C.: Improving minimum detectable differences in the assessment of soil organic matter](https://doi.org/10.1002/jpln.201400409)  
589 [change in short-term field experiments, \*J. Plant Nutr. Soil Sci.\*, 178, 35–42, <https://doi.org/10.1002/jpln.201400409>, 2015.](https://doi.org/10.1002/jpln.201400409)
- 590 Köchy, M., Hiederer, R., and Freibauer, A.: Global distribution of soil organic carbon – Part 1: Masses and frequency  
591 distributions of SOC stocks for the tropics, permafrost regions, wetlands, and the world, *SOIL*, 1, 351–365,  
592 <https://doi.org/10.5194/soil-1-351-2015>, 2015.

- 593 Lal, R., Negassa, W., and Lorenz, K.: Carbon sequestration in soil, *Current Opinion in Environmental Sustainability*, 15, 79–  
594 86, <https://doi.org/10.1016/j.cosust.2015.09.002>, 2015.
- 595 Laurila, T., Tuovinen, J.-P., Lohila, A., Hatakka, J., Aurela, M., Thum, T., Pihlatie, M., Rinne, J., and Vesala, T.: Measuring  
596 methane emissions from a landfill using a cost-effective micrometeorological method: MEASURING METHANE  
597 EMISSIONS, *Geophys. Res. Lett.*, 32, n/a-n/a, <https://doi.org/10.1029/2005GL023462>, 2005.
- 598 Lloyd, J. and Taylor, J. A.: On the Temperature Dependence of Soil Respiration, *Functional Ecology*, 8, 315,  
599 <https://doi.org/10.2307/2389824>, 1994.
- 600 Mattila, T.: Carbon action MULTA Finnish carbon sequestration experimental field dataset 2019,  
601 <https://doi.org/10.5281/ZENODO.3670654>, 2020.
- 602 Mattila, T. J., Hagelberg, E., Söderlund, S., and Joona, J.: How farmers approach soil carbon sequestration? Lessons learned  
603 from 105 ~~Carbon Farming Plans.~~ Paper submitted to carbon-farming plans, *Soil and Tillage Research*, 215, 105204,  
604 <https://doi.org/10.1016/j.still.2021.105204>, 2022.
- 605 Mattila, Tuomas and Heinonen, Reija: Carbon action MULTA Finnish carbon sequestration experimental field dataset 2020,  
606 <https://doi.org/10.5281/ZENODO.4068271>, 2021.
- 607 McMillen, R. T.: An eddy correlation technique with extended applicability to non-simple terrain, *Boundary-Layer Meteorol.*,  
608 43, 231–245, <https://doi.org/10.1007/BF00128405>, 1988.
- 609 Meersmans, J., Van Wesemael, B., De Ridder, F., Fallas Dotti, M., De Baets, S., and Van Molle, M.: Changes in organic  
610 carbon distribution with depth in agricultural soils in northern Belgium, 1960–2006: CHANGES IN SOC OF NORTHERN  
611 BELGIUM, 15, 2739–2750, <https://doi.org/10.1111/j.1365-2486.2009.01855.x>, 2009.
- 612 Merante, P., Dibari, C., Ferrise, R., Sánchez, B., Iglesias, A., Lesschen, J. P., Kuikman, P., Yeluripati, J., Smith, P., and Bindi,  
613 M.: Adopting soil organic carbon management practices in soils of varying quality: Implications and perspectives in Europe,  
614 *Soil and Tillage Research*, 165, 95–106, <https://doi.org/10.1016/j.still.2016.08.001>, 2017.
- 615 Minasny, B., Malone, B. P., McBratney, A. B., Angers, D. A., Arrouays, D., Chambers, A., Chaplot, V., Chen, Z.-S., Cheng,  
616 K., Das, B. S., Field, D. J., Gimona, A., Hedley, C. B., Hong, S. Y., Mandal, B., Marchant, B. P., Martin, M., McConkey, B.  
617 G., Mulder, V. L., O'Rourke, S., Richer-de-Forges, A. C., Odeh, I., Padarian, J., Paustian, K., Pan, G., Poggio, L., Savin, I.,  
618 Stolbovoy, V., Stockmann, U., Sulaeman, Y., Tsui, C.-C., Vågen, T.-G., van Wesemael, B., and Winowiecki, L.: Soil carbon  
619 4 per mille, *Geoderma*, 292, 59–86, <https://doi.org/10.1016/j.geoderma.2017.01.002>, 2017.
- 620 Oldfield, E. E., Wood, S. A., and Bradford, M. A.: Direct effects of soil organic matter on productivity mirror those observed  
621 with organic amendments, *Plant Soil*, 423, 363–373, <https://doi.org/10.1007/s11104-017-3513-5>, 2018.

622 Pastorello, G., Trotta, C., Canfora, E., Chu, H., Christianson, D., Cheah, Y.-W., Poindexter, C., Chen, J., Elbashandy, A.,  
623 Humphrey, M., Isaac, P., Polidori, D., Reichstein, M., Ribeca, A., van Ingen, C., Vuichard, N., Zhang, L., Amiro, B., Ammann,  
624 C., Arain, M. A., Ardö, J., Arkebauer, T., Arndt, S. K., Arriga, N., Aubinet, M., Aurela, M., Baldocchi, D., Barr, A.,  
625 Beamesderfer, E., Marchesini, L. B., Bergeron, O., Beringer, J., Bernhofer, C., Berveiller, D., Billesbach, D., Black, T. A.,  
626 Blanken, P. D., Bohrer, G., Boike, J., Bolstad, P. V., Bonal, D., Bonnefond, J.-M., Bowling, D. R., Bracho, R., Brodeur, J.,  
627 Brümmer, C., Buchmann, N., Burban, B., Burns, S. P., Buysse, P., Cale, P., Cavagna, M., Cellier, P., Chen, S., Chini, I.,  
628 Christensen, T. R., Cleverly, J., Collalti, A., Consalvo, C., Cook, B. D., Cook, D., Coursolle, C., Cremonese, E., Curtis, P. S.,  
629 D'Andrea, E., da Rocha, H., Dai, X., Davis, K. J., Cinti, B. D., Grandcourt, A. de Ligne, A. D., De Oliveira, R. C., Delpierre,  
630 N., Desai, A. R., Di Bella, C. M., Tommasi, P. di Dolman, H., Domingo, F., Dong, G., Dore, S., Duce, P., Dufrêne, E., Dunn,  
631 A., Dušek, J., Eamus, D., Eichelmann, U., ElKhidir, H. A. M., Eugster, W., Ewenz, C. M., Ewers, B., Famulari, D., Fares, S.,  
632 Feigenwinter, I., Feitz, A., Fensholt, R., Filippa, G., Fischer, M., Frank, J., Galvagno, M., et al.: The FLUXNET2015 dataset  
633 and the ONEFlux processing pipeline for eddy covariance data, *Scientific Data*, 7, 225, [https://doi.org/10.1038/s41597-020-](https://doi.org/10.1038/s41597-020-0534-3)  
634 [0534-3](https://doi.org/10.1038/s41597-020-0534-3), 2020.

635 Qu, Z., Oumbe, A., Blanc, P., Espinar, B., Gesell, G., Gschwind, B., Klüser, L., Lefèvre, M., Saboret, L., Schroedter-  
636 Homscheidt, M., and Wald, L.: Fast radiative transfer parameterisation for assessing the surface solar irradiance: The  
637 Heliosat-4 method, *Meteorol Z*, 26, 33–57, <https://doi.org/10.1127/metz/2016/0781>, 2017.

638 [Petchey, O. L., Pontarp, M., Massie, T. M., Kéfi, S., Ozgul, A., Weilenmann, M., Palamara, G. M., Altermatt, F., Matthews,](https://doi.org/10.1111/ele.12443)  
639 [B., Levine, J. M., Childs, D. Z., McGill, B. J., Schaepman, M. E., Schmid, B., Spaak, P., Beckerman, A. P., Pennekamp, F.,](https://doi.org/10.1111/ele.12443)  
640 [and Pearse, I. S.: The ecological forecast horizon, and examples of its uses and determinants, \*Ecol Lett\*, 18, 597–611,](https://doi.org/10.1111/ele.12443)  
641 <https://doi.org/10.1111/ele.12443>, 2015.

642 Rebmann, C., Kolle, O., Heinesch, B., Queck, R., Ibrom, A., and Aubinet, M.: Data Acquisition and Flux Calculations, in:  
643 *Eddy Covariance*, edited by: Aubinet, M., Vesala, T., and Papale, D., Springer Netherlands, Dordrecht, 59–83,  
644 [https://doi.org/10.1007/978-94-007-2351-1\\_3](https://doi.org/10.1007/978-94-007-2351-1_3), 2012.

645 Reichstein, M., Falge, E., Baldocchi, D., Papale, D., Aubinet, M., Berbigier, P., Bernhofer, C., Buchmann, N., Gilmanov, T.,  
646 Granier, A., Grunwald, T., Havrankova, K., Ilvesniemi, H., Janous, D., Knohl, A., Laurila, T., Lohila, A., Loustau, D.,  
647 Matteucci, G., Meyers, T., Miglietta, F., Ourcival, J.-M., Pumpanen, J., Rambal, S., Rotenberg, E., Sanz, M., Tenhunen, J.,  
648 Seufert, G., Vaccari, F., Vesala, T., Yakir, D., and Valentini, R.: On the separation of net ecosystem exchange into assimilation  
649 and ecosystem respiration: review and improved algorithm, *Global Change Biol*, 11, 1424–1439,  
650 <https://doi.org/10.1111/j.1365-2486.2005.001002.x>, 2005.

651 Richardson, A. D., Mahecha, M. D., Falge, E., Kattge, J., Moffat, A. M., Papale, D., Reichstein, M., Stauch, V. J., Braswell,  
652 B. H., Churkina, G., Kruijt, B., and Hollinger, D. Y.: Statistical properties of random CO<sub>2</sub> flux measurement uncertainty  
653 inferred from model residuals, *Agricultural and Forest Meteorology*, 148, 38–50,  
654 <https://doi.org/10.1016/j.agrformet.2007.09.001>, 2008.

- 655 Saby, N. P. A., Arrouays, D., Antoni, V., Lemerrier, B., Follain, S., Walter, C., and Schwartz, C.: Changes in soil organic  
656 carbon in a mountainous French region, 1990-2004, 24, 254–262, <https://doi.org/10.1111/j.1475-2743.2008.00159.x>, 2008.
- 657 Sanderman, J., Hengl, T., and Fiske, G. J.: Soil carbon debt of 12,000 years of human land use, Proc Natl Acad Sci USA, 114,  
658 9575–9580, <https://doi.org/10.1073/pnas.1706103114>, 2017.
- 659 [Scharf, P. C., Shannon, D. K., Palm, H. L., Sudduth, K. A., Drummond, S. T., Kitchen, N. R., Mueller, L. J., Hubbard, V. C.,](#)  
660 [and Oliveira, L. F.: Sensor-Based Nitrogen Applications Out-Performed Producer-Chosen Rates for Corn in On-Farm](#)  
661 [Demonstrations, Agron.j., 103, 1683–1691, https://doi.org/10.2134/agronj2011.0164, 2011.](#)
- 662 [Sela, S., Woodbury, P. B., and van Es, H. M.: Dynamic model-based N management reduces surplus nitrogen and improves](#)  
663 [the environmental performance of corn production, Environ. Res. Lett., 13, 054010, https://doi.org/10.1088/1748-](#)  
664 [9326/aab908, 2018.](#)
- 665 Smith, P., Soussana, J., Angers, D., Schipper, L., Chenu, C., Rasse, D. P., Batjes, N. H., Egmond, F., McNeill, S., Kuhnert,  
666 M., Arias-Navarro, C., Olesen, J. E., Chirinda, N., Fornara, D., Wollenberg, E., Álvaro-Fuentes, J., Sanz-Cobena, A., and  
667 Klumpp, K.: How to measure, report and verify soil carbon change to realize the potential of soil carbon sequestration for  
668 atmospheric greenhouse gas removal, Glob Change Biol, 26, 219–241, <https://doi.org/10.1111/gcb.14815>, 2020.
- 669 VandenBygaart, A. J. and Angers, D. A.: Towards accurate measurements of soil organic carbon stock change in  
670 agroecosystems, Can. J. Soil. Sci., 86, 465–471, <https://doi.org/10.4141/S05-106>, 2006.
- 671 [Viskari, T., Laine, M., Kulmala, L., Mäkelä, J., Fer, I., and Liski, J.: Improving Yasso15 soil carbon model estimates with](#)  
672 [ensemble adjustment Kalman filter state data assimilation, Geosci. Model Dev., 13, 5959–5971, https://doi.org/10.5194/gmd-](#)  
673 [13-5959-2020, 2020.](#)
- 674 Webb, E. K., Pearman, G. I., and Leuning, R.: Correction of flux measurements for density effects due to heat and water  
675 vapour transfer, Q.J Royal Met. Soc., 106, 85–100, <https://doi.org/10.1002/qj.49710644707>, 1980.
- 676 Weiss, M. and Baret, F.: S2toolbox Level 2 Products: Lai, Fapar, Fcover, 2016.
- 677 White, J. W., Hunt, L. A., Boote, K. J., Jones, J. W., Koo, J., Kim, S., Porter, C. H., Wilkens, P. W., and Hoogenboom, G.:  
678 Integrated description of agricultural field experiments and production: The ICASA Version 2.0 data standards, Computers  
679 and Electronics in Agriculture, 96, 1–12, <https://doi.org/10.1016/j.compag.2013.04.003>, 2013.